A Non-Scaling Radial-Sector Fixed Field Alternating Gradient (FFAG) Ring for Carbon Cancer Therapy

Eberhard Keil[*], Andrew Sessler[†] and Dejan Trbojevic[**]

[*]*CERN, CH1211 Geneva 23, Switzerland*
[†]*Lawrence Berkeley National Laboratory, Berkeley CA 29720, USA*
[**]*Brookhaven National Laboratory, Upton NY 11973, USA*

Abstract. A non-scaling radial-sector FFAG is investigated as a machine to produce 2×10^9 particles of C^{6+} per pulse, at an energy of 400 MeV. This is accomplished by having an ECR ion source (producing C^{4+} at 40 keV per nucleon), followed by an RFQ (that accelerates to a few MeV/u) and then a rapidly cycling synchrotron or linac that takes the carbon ions from 1 MeV/u to 31 MeV/u. The carbon is then fully stripped and accelerated in one FFAG to 119 MeV/u and then in a second FFAG to 414 MeV/u. The top FFAG has a radius of only 8.1 m and an aperture of 20 cm. The magnets are superconducting and have a maximum pole tip field of 5.3 T. The fields are linear, so the dynamic aperture is large. On the other hand, because the FFAG is non-scaling the tunes vary during acceleration and the rate of acceleration must be rapid enough to pass through resonances without unacceptable degradation of the beam.

Keywords: Cyclotron, cancer hadron therapy, FFAG cyclotron
PACS: 29.20.Hm, 29.27.Eg, 41.75.Ak, 41.85.Lc, 87.56.By

INTRODUCTION

A very interesting study of a series of scaling radial-sector FFAGs (three machines) for carbon cancer therapy has been undertaken by Misu et al.[1]. The interest in FFAG machines arises because of the medical interest in the latest therapy technique of spot-scanning which requires (about) 200Hz repetition rate which can not be achieved with a conventional synchrotron[2].

The major difficulties, encountered by Misu et al with the use of scaling FFAGs were:

1. The radius of the top FFAG is rather large (11 m).
2. The aperture of magnets is rather large (65 cm).
3. The dynamic aperture in the low energy FFAG is rather small (80% of the beam is lost during acceleration).
4. The rf frequency is forced to be rather low (in the megahertz range so as to cover the aperture).

In this contribution we develop a scheme that overcomes these difficulties. We propose the same ECR ion source, but then follow it immediately with an RFQ that accelerates the ions to a few MeV/u. Then we invoke a rapidly cycling synchrotron, operating at 200 Hz, or a linac, to accelerate from the output of the RFQ to 31 MeV/u. It should not be difficult to cycle the synchrotron so rapidly as the top energy is very small and, hence, the inductance of the synchrotron magnets is greatly reduced from earlier machines that operated at 60 Hz and went to a few GeV. Then, we propose two non-scaling FFAGs that operate over a range, in each, where the ion momentum changes by a factor of two. By the use of superconducting magnets we address difficulty no. 1. The non-scaling (in contrast with a scaling) FFAG addresses difficulty no. 2. A non-scaling FFAG is almost linear and hence has a large dynamic aperture, so difficulty no. 3 is addressed (but not actually used in this design as we propose a synchrotron or linac (not an FFAG) at low energy (where the losses were large in the Misu et al design). Finally, because the aperture is reduced, compared with the Misu et al design, higher frequency rf may be employed.

---

[1] e-mail Eberhard.Keil@t-online.de
[2] e-mail AMSessler@lbl.gov
[3] Supported by the U.S. Department of Energy under Contract No. DE-AC03-76SF0009
[4] e-mail Trbojevic@bnl.gov
[5] Supported by the U.S. Department of Energy under Contract No. DE-AC02-98CH10886

The ”down-side” of a non-scaling FFAG is that the tune varies during acceleration and, therefore, transverse resonances must be crossed. We explore this subject and determine the necessary rate of acceleration so as not to unacceptably disturb the ion beam. We design the machine not to cross the intrinsic half integral resonance (although the third and higher order resonances are crossed), but machine resonances (imperfection resonances) of all orders are crossed. This then puts a restriction on a combination of the magnet imperfections and the rate of acceleration.

TABLE 1. FFAG Ring Parameters

Parameter	Ring 1	Ring 2
Injection energy E_{inj}/u (MeV)	31.1	119
Extraction energy E_{ext}/u (MeV)	119	414
Number of periods	25	25
Period length (m)	1.36	2.04
Circumference (m)	34	51

FFAG LATTICE

The parameters of the two FFAG rings, presented in Table 1, are derived from those of two FFAG rings[3], which accelerate protons from 20 to 77 MeV, and from 77 to 250 MeV kinetic energy, respectively. The reference orbit is taken at injection. The ratio of the momenta at extraction and injection is exactly two. Hence, acceleration happens between relative momentum errors $\Delta p/p = 0$ at injection and $\Delta p/p = 1$ at extraction. The lengths of the elements and the periods, and the circumference of Ring 2 are 3/2 of those in Ring 1, thus permitting the installation of Ring 2 around Ring 1.

The cell parameters are shown in Table 2. The lengths, bending angles, magnetic fields and gradients are taken on the reference orbit. The pole tip fields are taken at the pole tip, as will be discussed below. By design, the reference momentum in Ring 2 is twice that in Ring 1. It follows that the magnetic fields in Ring 2 are 4/3 of those in Ring 1, and that the magnetic gradients in Ring 2 are 8/9 of those in Ring 1.

TABLE 2. FFAG Cell Parameters

Parameter	Ring 1	Ring 2
F magnet length (m)	0.14	0.21
F magnet bending angle	-0.04854	-0.04854
F magnet field (T)	-0.563	-0.751
F magnet gradient (T/m)	34.2	30.4
D magnet length (m)	0.3	0.45
D magnet bending angle	0.3484	0.3484
D magnet field (T)	1.89	2.51
D magnet gradient (T/m)	-27.4	-24.3
Short straight section length (m)	0.08	0.12
Long straight section length (m)	0.62	0.93

Table 3 gives the beam parameters as calculated by the PTC_TWISS command in madX[4]. All parameters with dimension metres scale like the scale factor 3/2 between Ring 2 and Ring 1. File names and excessive digits will be removed at the last moment. Figure 1 shows the orbit functions β_x, β_y and the dispersion D_x in a cell of Ring 1 at the reference momentum.

Fig. 2 shows the variation of the phase advances with the relative momentum error $\Delta p/p$ for both rings. The phase advances at $\Delta p/p = 0$ are design parameters, those for $\Delta p/p > 0$ are the result of a calculation with PTC_TWISS. Fig. 2 also shows the variation of the maximum β-functions with the relative momentum error $\Delta p/p$ for Ring 2. They are the result of a calculation with PTC_TWISS. In Ring 1, the maximum β-functions are 2/3 of those shown.

Beam Size, Aperture and Pole Tip Field

The RMS beam radii follow from emittance, momentum and β-functions. They are displayed in Table 4. Following Misu et al., we assume 1 mm normalised emittance at 400 MeV/u and scale from there. In the aperture, we allow for three RMS beam radii. Three contributions add to the full horizontal aperture: 3 beam radii at injection − reference

TABLE 3. Beam Parameters from PTC_TWISS in madX

Parameter	Ring 1	Ring 2
Radial swing of equilibrium orbit (m)	0.1248	0.1873
H Phase advance per cell at injection	0.3500	0.3500
V Phase advance per cell at injection	0.3500	0.3500
H Phase advance per cell at extraction	0.1461	0.1461
V Phase advance per cell at extraction	0.1228	0.1228
Maximum H beta at injection (m)	1.0141	1.5212
Maximum V beta at injection (m)	3.5764	5.3646
Maximum H beta at extraction (m)	0.9452	1.4178
Maximum V beta at extraction (m)	1.5414	2.3120
Maximum H dispersion at injection (m)	0.0620	0.0931
Maximum H dispersion at extraction (m)	0.2574	0.3861

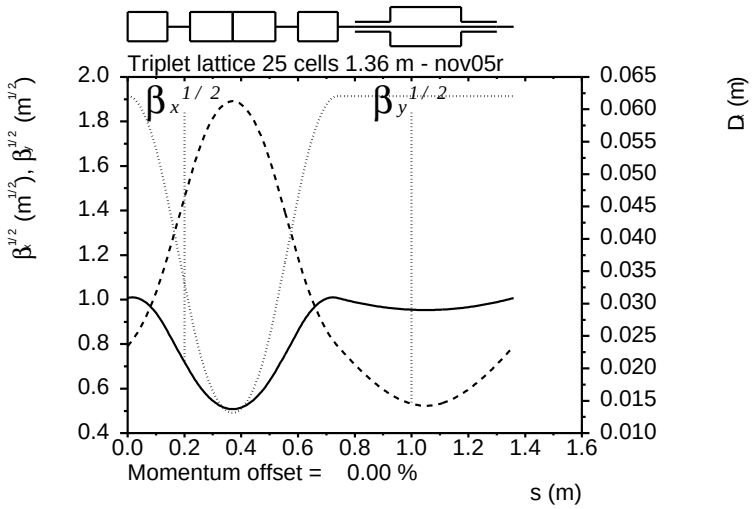

FIGURE 1. Orbit functions in a cell of Ring 1; full line horizontal $\sqrt{\beta_x}$ in $\sqrt{m}$, dashed line vertical $\sqrt{\beta_y}$ in $\sqrt{m}$, dotted line horizontal dispersion D_x in metres. In Ring 2, $\sqrt{\beta_x}$ and $\sqrt{\beta_y}$ are a factor $\sqrt{3/2}$ larger, and D_x is a factor 3/2 larger than in Ring 1.

orbit – the radial swing of the equilibrium orbit, and 3 beam radii at extraction. The position of the horizontal aperture with respect to the reference orbit is as shown. The swing of the horizontal closed orbit between injection and extraction is much larger than the horizontal beam radii. If we allow approximately 4 mm for closed orbit distortions, we arrive at the apertures shown in Table 4. The magnets are super-imposed dipoles and quadrupoles. We calculate the magnetic

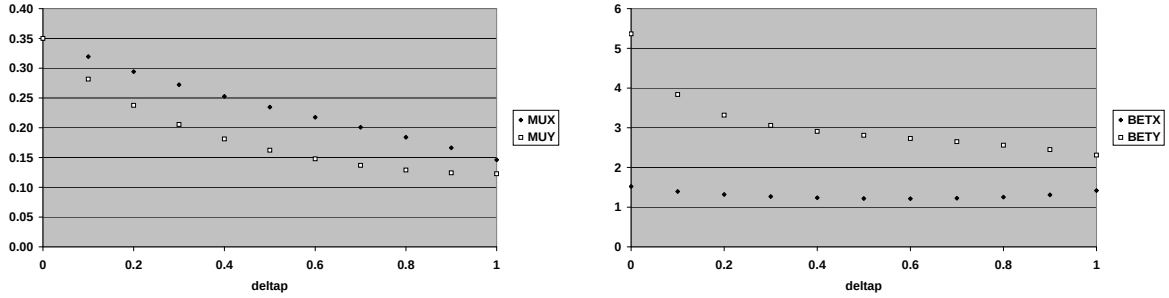

FIGURE 2. Parameter variations with the relative momentum error $\Delta p/p$. The horizontal and vertical phase advances μ_x and μ_y through a lattice cell, measured in cycles, in both rings are on the left. The horizontal and vertical functions β_x and β_y in metres in Ring 2 are on the right. In Ring 1 β_x and β_y are 2/3 of those in Ring 2.

field at both edges of the horizontal aperture, define the pole tip field as the larger of the two in absolute value, and display it in Table 4. These pole tip fields are within the reach of super-conducting magnets.

TABLE 4. Beam Size, Aperture and Pole Tip Field

Parameter	Ring 1	Ring 2
Emittance at injection (μm)	4	2
Emittance at extraction (μm)	2	1
Max H beam radius at injection (mm)	2.0141	1.7442
Max H beam radius at extraction (mm)	1.3749	1.1907
Max V beam radius at injection (mm)	3.7823	3.2756
Max V beam radius at extraction (mm)	1.7558	1.5206
H aperture (mm)	$-10\ldots+133$	$-9\ldots+195$
V aperture (mm)	± 15	± 14
D magnet pole tip field (T)	2.2	2.7
F magnet pole tip field (T)	4.0	5.2

Design of the RF system

Table 5 shows parameters related to the design of the RF system. The circumference of Ring 1 at injection has the design value already shown in an earlier table, that of Ring 2 is exactly 3/2 of the extraction orbit in Ring 1. The circumferences at extraction are larger than those at injection, because the extraction orbits are outside the injection orbits on the whole circumference. The speeds in units of the light velocity follow from the injection and extraction energies. The revolution frequencies follow from the circumferences and the speeds. They vary by almost a factor of two. The harmonic numbers h are integers and design parameters yet to be fixed. That in Ring 2 is 3/2 of that in Ring 1, in order to allow bunch to bucket transfer from Ring 1 to Ring 2. Hence, the harmonic number in Ring 1 must be even. The two RF systems should be locked in phase during the transfer. The RF frequencies are simply the products of h and the revolution frequencies. In Ring 1, we find the harmonic number h and the circumferential voltage V_{RF} from the requirement, that the bucket height Δ_b in terms of $\Delta p/p_r$ and the invariant bucket area A_b at injection are larger than the assumed values $\Delta_b = 0.01$ and $A_b = 0.5$ eVs. In Ring 2, we adjust V_{RF} such that we get $\Delta_b = 0.01$, and observe that A_b becomes larger than in Ring 1. The RF frequencies are simply the products of h and the revolution frequencies.

TABLE 5. Parameters of the RF system

Parameter	Ring 1	Ring 2
Circumference at injection C_i (m)	34	51.932
Circumference at extraction C_e (m)	34.621	52.863
Speed at injection β_i	0.2511	0.4606
Speed at extraction β_e	0.4606	0.7201
Revolution frequency at injection f_i (MHz)	2.215	2.659
Revolution frequency at extraction f_e (MHz)	3.989	4.084
Stable phase angle φ_s	0.04π	0.04π
Harmonic number h	6	9
Circumferential RF voltage V_{RF} (MV)	0.1592	0.6162
Actual energy gain/turn (keV)	119.7	463.4
RF frequency at injection f^i_{RF} (MHz)	13.293	23.932
RF frequency at extraction f^e_{RF} (MHz)	23.932	36.755
Bucket height at injection Δ_b	0.0109	0.0100
Bucket area at injection A_b (eVs)	0.6536	1.2178
Max acceleration time T_a (ms)	5	5
Max number of turns at β_i	11072	13538
Min energy gain/turn (keV)	7.9	21.8

The relation between acceleration time T_a and repetition frequency f_r is $T_a \leq 1/f_r$. At $f_r = 200$ Hz we have $T_a \leq 5$ ms. The number of turns for acceleration is $N_a = T_a \beta c/C$. Here β is the relativistic factor, which varies during acceleration, c is the speed of light, and C is the circumference. Ignoring the variation of β during acceleration, and using its value at injection β_i, we find the number of turns displayed in Tab. 5. We assume that the RF system operates

at constant voltage and accelerates by the same energy step on each turn. The energy gain in a turn is $(E_f - E_i)/N_a$ with final energy E_f and initial energy E_i, and is also shown in Tab. 5. Although the C^{6+} ions are accelerated with nearly stationary buckets at a very small stable phase angle φ_s, the actual energy gain/turn is much larger than the minimum energy gain/turn, and the actual number of turns is much smaller than the maximum. Hence, our estimates of the tune change per turn are pessimistic.

Resonance crossing

The tunes Q_x and Q_y vary between $Q_x = Q_y = 8.75$ at injection and $Q_y \approx 3$ at extraction, and hence straddle a range of about six units. Neglecting variations, the tune change per turn is at least $Q_\tau = 6/N_a = 4 \times 10^{-4}$. In order to estimate the effect on the geometrical emittance ε, we employ the standard formulae summarized by R. Bartman[5], who attributes the following formula to G. Guignard for the m-th order resonance $mQ_x = n$:

$$\left| \frac{\Delta(\varepsilon^{1-m/2})}{m-2} \right| = \frac{\pi}{\sqrt{mQ_\tau}} \frac{R}{2^{m-2} B\rho} \left| \frac{1}{2\pi} \int_0^{2\pi} \frac{\beta_x^{m/2}}{(m-1)!} \frac{\partial^{m-1} B_z}{\partial x^{m-1}} \exp(in\theta) \mathrm{d}\theta \right| \tag{1}$$

Here R is the average radius, $B\rho$ the magnetic rigidity of the C^{6+} ions. The term $|\ldots|$ on the right hand side is the n-th Fourier component of the $(m-1)$-th derivative of the magnetic field B_z, weighted with the horizontal β-function to the power $m/2$. For small enough emittance blow-up $\Delta\varepsilon/\varepsilon \ll 1$, we can expand (1) and write it in the form:

$$\left| \frac{\Delta\varepsilon}{\varepsilon} \right| = \frac{\varepsilon^{m/2-1}}{\sqrt{mQ_\tau}} \frac{C}{2^{m-2} B\rho} \left| \frac{1}{2\pi} \int_0^{2\pi} \frac{\beta_x^{m/2}}{(m-1)!} \frac{\partial^{m-1} B_z}{\partial x^{m-1}} \exp(in\theta) \mathrm{d}\theta \right| \tag{2}$$

Here C is the circumference. We first apply (2) to the intrinsic or systematic resonances $mQ_x = N_p$ or $\mu_x = 1/m$ with $3 \le m \le 6$, which are crossed during acceleration. Here $N_p = 25$ is the number of lattice periods. For the third-order resonance $3Q_x = 25$ in Ring 1, we find with C from Tab. 1, the length of the two F magnets from Tab. 2, ε from Tab. 4, and $B\rho = 1.625$ Tm, that $|\partial^2 B_z/\partial x^2| < 0.6$ T/m^2. This corresponds to a field error of order 10^{-3} at the edge of the aperture. The tolerable field components $|\partial^{m-1} B_z/\partial x^{m-1}|$ of the intrinsic resonances of order $m > 3$ are larger by about a factor $1/\sqrt{\varepsilon} \approx 50$ for every increase of m by one, since $\beta_x \approx 1$ m.

Five integer resonances and eleven half-integer are crossed in the course of acceleration. These resonances are only driven by errors. For the integral resonances the growth in betatron amplitude A amplitude in smooth approximation is given by:

$$\Delta A = \frac{\pi \overline{R} B_n}{\overline{B} Q \sqrt{Q_\tau}} = \frac{C}{2Q\sqrt{Q_\tau}} \frac{B_n}{\overline{B}} \tag{3}$$

Here $\overline{R}$ and $\overline{B}$ are average radius and average magnetic field, B_n is the n-th Fourier component of the vertical magnetic field B, Q is the tune, Q_τ is the tune change per turn, and C is the circumference. The second form can conveniently be solved for the ratio $B_n/\overline{B}$. The condition is tighter in the larger ring. Assuming $\Delta A/A = 0.1$ and the other parameters as already listed, we find $B_n/\overline{B} \le 3.4\ 10^{-4}$. For half-integral resonances, which are also only driven by errors, the growth in betatron amplitude A is in smooth approximation:

$$\log \frac{A_e}{A_i} = \frac{\pi}{\sqrt{2Q_\tau}} \frac{\overline{R}}{2\overline{B}} \frac{\partial B_n}{\partial x} = \frac{C}{4\overline{B}\sqrt{2Q_\tau}} \frac{\partial B_n}{\partial x} \tag{4}$$

Taking $\Delta A/A = 0.1$, and the other parameters as already listed, we find with $\overline{B} \approx 0.4$ T, that $|\partial B_n/\partial x| \le 2.2\ 10^{-4}$ T/m.

The tolerances for the field components are tight. They could be relaxed by about an order of magnitude, by allowing a larger blow-up in emittance and betatron amplitude, and by crossing the resonances more quickly. The RF voltage is large enough to allow faster resonance crossing, since it is determined by bucket height and area, rather than the rate of acceleration.

COMMENTS

Further work that needs to be done includes a careful study of non-linear effects and the emittance blow-up associated with resonance crossing by simulation. Of course, the simple work here must be augmented with engineering studies and, then, with cost estimates.

Our machines have the property that the reference orbit enters and leaves the magnets at a right angle with respect to the magnet end faces. Hence, they are not strictly radial-sector FFAG rings, because the magnet end faces do not point towards the machine centre. Spiral-sector FFAG rings might be an attractive alternative.

CONCLUSION

There are good medical reasons for using a cyclotron for medical therapy; namely the use of spot-scanning which can not be achieved with a synchrotron. In this paper we have shown that two non-scaling FFAG cyclotrons in cascade can be used as the central elements of a carbon therapy cancer center. Our result strongly motivates further theoretical investigations, engineering studies, and cost estimates.

REFERENCES

1. Misu, T. et al, Phys. Rev. Special Topics: Accelerators and Beams **7** (2004) 094701.
2. Spot scanning web page: http://radmed.web.psi.ch/asm/gantry/conclu/n_conclu.html
3. Trbojevic, D. et al, ”Design of a non-scaling FFAG accelerator for proton therapy”, submitted to the Proceeding of Cyclotron 2004 (2004).
4. madX web page: http://mad.home.cern.ch/mad/
5. Baartman, R.,”Fast crossing of betatron resonance”, presented at the FFAG Workshop, Vancouver (2004); Guignard, G., CERN Report 77-10 (1977).